Plasma Physics Reports, Vol. 26, No. 9, 2000, pp. 792–800. Translated from Fizika Plazmy, Vol. 26, No. 9, 2000, pp. 845–853.

LOW-TEMPERATURE PLASMA

Sterilization of Medical Products in Low-Pressure Glow Discharges

I. A. Soloshenko*, V. V. Tsiolko*, V. A. Khomich*, A. I. Shchedrin*, A. V. Ryabtsev*, V. Yu. Bazhenov*, and I. L. Mikhno**

**Institute of Physics, National Academy of Sciences of Ukraine, pr. Nauki 1444, Kiev, 03039 Ukraine*

***Institute of Epidemiology and Infectious Diseases, Ministry of Health of Ukraine, Ukraine*

Received June 22, 1999; in final form, December 25, 1999

Abstract—Results are presented from experimental and theoretical studies of the sterilization of medical products by the plasmas of dc glow discharges in different gas media. The sterilization efficiency is obtained as a function of discharge parameters. The plasma composition in discharges in N_2 and O_2 is investigated under the operating conditions of a plasma sterilizer. It is shown that free surfaces of medical products are sterilized primarily by UV radiation from the discharge plasma, while an important role in sterilization of products with complicated shapes is played by such chemically active particles as oxygen atoms and electronically excited O_2 molecules. © *2000 MAIK "Nauka/Interperiodica".*

1. INTRODUCTION

In present-day medical practice, there is a need for cold sterilization of many thermolabile instruments and materials. Up to now, these medical products have been surface-sterilized by toxic gases such as ethylene oxide and its mixtures with chlorofluorocarbons. However, the products sterilized in this way should be aerated over a long period (up to 24 hours); moreover, they are very dangerous for the health of the involved staff and are environmentally unfriendly. In this connection, it becomes highly relevant to develop new methods for cold sterilization. One of the most important present-day alternatives to gaseous sterilization is sterilization by gas-discharge plasmas. The main advantage of the plasma sterilization technique is that the plasma, being a chemically active medium, is created during the processes of excitation, dissociation, and ionization of any gas or vapor plasma-producing media (including nontoxic media and even inert gases). Chemically active particles exist only in the course of the discharge and disappear practically instantaneously after the discharge is switched off. These two circumstances make it possible to completely solve safety and ecological problems.

Although the idea of sterilizing medical products by gas-discharge plasmas was originated as early as the 1960s [1, 2], the efficiency of this method and the boundaries of its applicability have not been examined in detail up to now. Some aspects of this complicated problem were discussed in [3–7].

Here, we report on experimental and theoretical investigations of the physical processes that govern the efficiency of sterilization by a low-pressure gas-discharge plasma. We also describe relevant medical and biological tests. The results obtained answer the questions regarding the effectiveness of the plasma sterilization method and the boundaries of its applicability when gases that are the most interesting from a practical standpoint (air, oxygen, hydrogen, carbon dioxide, nitrogen, and argon) are used.

2. EXPERIMENTAL LAYOUT AND STERILIZATION TECHNIQUES

In our experiments, the plasma was created by dc glow discharges. The discharge current and voltage were varied over the ranges 0.05–0.7 A and 400–600 V; the working volume of the sterilization chamber ranged between 20 to 40 l. The working gases (the gases mentioned above or their mixtures) were admitted into the chamber pre-evacuated by a fore pump to a residual pressure of 3×10^{-3} torr. The working gas pressure was varied over the range from 5×10^{-2} to 25×10^{-2} torr. The plasma density and electron energy distribution function (EEDF) were measured by single and double Langmuir probes made of tungsten wires 50, 105, and 240 μm in diameter, the receiving sections being from 5 to 10 mm in length. The design of the probes allowed measurements over the entire chamber volume. In measuring the current–voltage (I–V) characteristics of the probes, the effects of discharge current pulsations were eliminated and the measurement accuracy was increased using the modified method described in [8]. The I–V characteristics of the probes were monitored with a specially devised programmable diagnostic system controlled by a personal computer. A complete cycle of measurements included 2048 steps, synchronized with the change in the supply voltage. Our method differed from the method of [8] in that, at each step of a measurement cycle, the controlling computer

1063-780X/00/2609-0792$20.00 © 2000 MAIK "Nauka/Interperiodica"

code specified the probe current with an accuracy of 0.1 μA and provided simultaneous measurements of the probe voltage relative to the anode, the anode voltage, and the discharge current. The results of measurements in the prescribed ranges of the discharge current and probe voltage were recorded as the dependence of the probe current on the probe voltage at a given discharge current and discharge voltage. The plasma density was computed from the electron saturation current, and the EEDF was evaluated by using special subroutines through differentiating the I–V characteristics twice [9] and preinterpolating (if necessary) the measured data. In the above pressure range, the plasma density was found to be essentially pressure-independent and was governed exclusively by the input power. With increasing the input power density W_d from 3×10^{-3} to 30×10^{-3} W/cm^3, the plasma density increased almost linearly from 7×10^8 to 6×10^9 cm^{-3} (Fig. 1, curve *1*), in which case the degree of plasma inhomogeneity in the working volume of the sterilization chamber was at most 25–30%. The EEDF was measured in discharges in air, oxygen, and nitrogen. In oxygen and air, the EEDF was found to be monotonic. In some regimes of a discharge in nitrogen, the EEDF was observed to be inverted in the energy range 2–4 eV because of the vibrational excitation of N_2 molecules (Fig. 2, curve *3*).

The electric field in the plasma volume is an important parameter of a gas discharge. We found that, under typical discharge conditions ($P = 4 \times 10^{-2} = 2 \times 10^{-1}$ torr and $W_d = 3 \times 10^{-3}$–25×10^{-3} W/cm^3), the electric field strength varied in a range from about 0.1 to about 1.0 V/cm. The related results of measurements in a nitrogen plasma are illustrated in Fig. 3.

The UV radiation power was monitored in the following two ways. In the wavelength band 220–320 nm, the UV power was measured by a DAU-81 apparatus. In the vacuum UV and soft UV spectral bands ($120 \le \lambda < 220$ nm), the radiation power was measured by a specially developed photoresist-based technique, which consisted of the following: the exposure time of a photoresist (i.e., the time over which the exposed photoresist disappeared entirely from the substrate surface in a specially prepared solution) was uniquely determined by the fraction of UV radiation absorbed by the photoresist. The substrates with a photoresist were exposed to UV radiation from a plasma over different times and were developed. Then, we plotted the so-called characteristic curves, showing the rate at which a photoresist disappeared versus the exposure time. A comparison between these characteristic curves and those obtained from experiments carried out with sources with known powers and UV radiation spectra allowed us to determine the power of UV radiation from the discharge plasma with a sufficiently high degree of confidence. We found that the radiation intensity increased with increasing the input power density W_d (Fig. 1, curve *2*) and that the bulk of the UV power, approximately W_s =

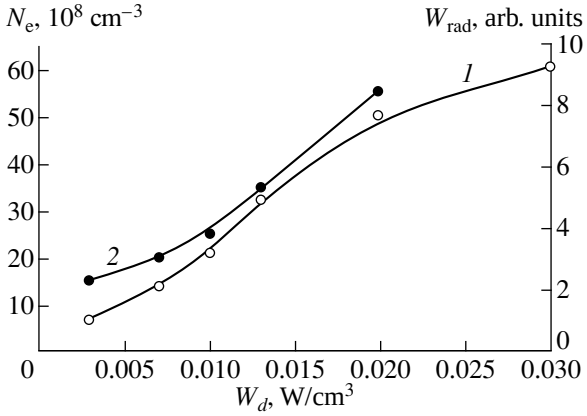

Fig. 1. (*1*) UV radiation flux density and (*2*) UV radiation power vs. the specific power input into a discharge in air at the pressure $P = 20 \times 10^{-2}$ torr.

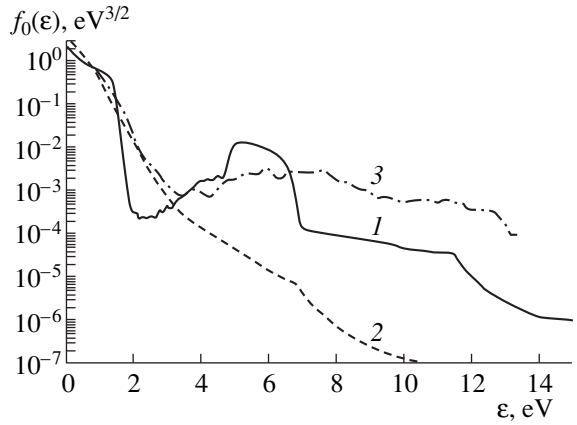

Fig. 2. Representative profiles of the EEDF calculated theoretically for (*1*) nitrogen and (*2*) oxygen and (*3*) the EEDF measured experimentally in a discharge plasma in nitrogen.

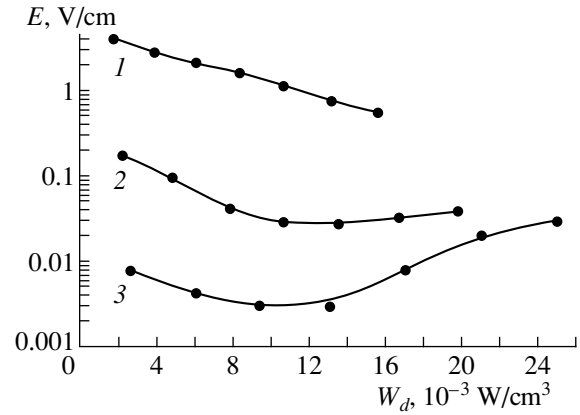

Fig. 3. Steady-state electric field in a plasma vs. the specific power input into discharges in nitrogen at different pressures P = (*1*) 2×10^{-1}, (*2*) 1×10^{-1}, and (*3*) 4×10^{-2} torr.

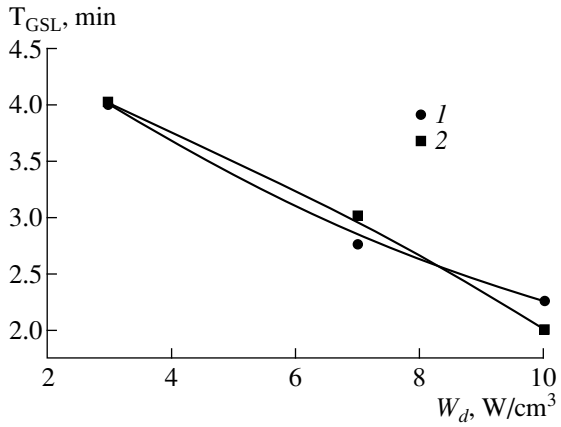

Fig. 4. Sterilization time T_{GSL} vs. the specific power input into discharges in air at two different pressures P = (*1*) 8×10^{-2} and (*2*) 20×10^{-2} torr, the initial surface density of the spores being 10^7 spore/cm^2.

50–100 μW/cm^2 at $W_d = (3–7) \times 10^{-3}$ W/cm^3, was emitted from the plasma at the wavelengths $\lambda \le 220$ nm.

The temperature of the sterilized products (test objects) was measured with a chromel–alumel thermocouple. The discharge regimes were chosen so that the temperature of the sterilized test objects was at most 60°C, in accordance with the requirements for sterilizing thermolabile materials.

As test objects, we used metal and glass Petri dishes with an inner surface area of about 10 cm^2. Medical and biological investigations were carried out with spores and with vegetative and viral microorganisms. The results reported below were obtained in experiments with the spores of Bacillus subtilis, which turned out to be the most resistant to sterilization by discharge plasmas. The inner surfaces of the Petri dishes were infected uniformly with spore-containing water suspensions. Initially, the number of spores on test objects varied between 10^5 to 10^8 (i.e., the mean surface density of the spores was 10^4–10^7 spore/cm^2). Note that the real density of microorganisms on the presterilized products is much lower (10^2–10^3 cm^{-2}); moreover, these are mostly vegetative microorganisms, which are substantially less resistant to sterilization in comparison with spores. In other words, the conditions under which we investigated sterilization by plasma were much more stringent than those prevailing in medical practice. After incubation of the spores on the test objects sterilized by plasma, we controlled the extent to which the objects were sterilized by immediately counting the number of colonies of the spores (i.e., the number of spores that survived the sterilization). Then, we plotted the survivability profiles, which reflected the number of microorganisms that remained alive versus the sterilization time. The sterilization efficiency was characterized by the time during which a guaranteed sterilization level (GSL) of 10^{-6} was achieved, i.e., the time T_{GSL} during which one of every 10^6 spores infected initially on the test objects survived the sterilization.

3. EXPERIMENTAL RESULTS

In our previous papers [6, 7] aimed at revealing the main features of sterilization by a low-pressure glow discharge plasma, we established the following:

(i) The sterilization time in discharges in all gases used in experiments is essentially independent of the gas pressure over the entire pressure range under investigation, $(8–25) \times 10^{-2}$ torr, and decreases with increasing the specific power input into the discharge (Fig. 4). Consequently, the efficiency of sterilization in discharges in each of the gases is determined by the plasma density.

(ii) The most efficient working gas is oxygen; less efficient gases in decreasing order are air, carbon dioxide, hydrogen, argon, and nitrogen.

(iii) The efficiency of sterilization by plasma decreases as the initial density of spores on the test objects is increased from 10^6 to 10^7 spore/cm^2. The reason is that, at densities of about 10^7 spore/cm^2, the spores stick together, forming lumps inside of which the spores are more resistant to plasma sterilization and thereby increase the sterilization time. Clearly, this feature of sterilization by plasma is characteristic of any plasma sterilizer.

Our main purpose here is to investigate the main sterilizing factors of low-temperature plasmas of low-pressure glow discharges: the charged plasma particles, UV radiation from the plasma, and chemically active neutral plasma particles (such as radicals and excited atoms and molecules).

To determine the relative efficiency of sterilization by charged plasma particles, we carried out experiments on the sterilization of metal test objects. Varying the potential applied to a test object, we were able to change the energy and intensity of the electron and ion fluxes onto the object, without changing the fluxes of chemically active neutral plasma particles or UV radiation from the plasma. If the charged particles play an important role in sterilization, then the sterilization efficiency should be very sensitive to the potential applied to test objects. We found that the survivability profiles obtained in experiments with metal test objects held at the anode, cathode, or floating potentials were essentially identical, thereby providing clear evidence that charged plasma particles did not affect the sterilization process.

To analyze the relative role of UV radiation from the discharge plasma, we carried out experiments with test objects that were sterilized either directly or through filters made of lithium fluoride (LiF) and a KU-1 quartz glass 3 mm thick. In the absence of filters, the objects were sterilized by the combined action of UV radiation

and chemically active neutral particles, while filter-protected objects were sterilized only by UV radiation of wavelengths $\lambda \geq 120$ nm (in the case of LiF filters) and $\lambda \geq 160$ nm (in the case of quartz filters). Figure 5 shows the survivability profiles for spores during sterilization by the combined action of UV radiation and active neutral particles and exclusively by UV radiation in discharge plasmas in oxygen, air, and nitrogen. We can see that, for these gases, the profiles characterizing sterilization with and without filters are practically identical. Similar results were obtained from experiments with filters made of a KU-1 quartz glass and LiF over the entire ranges of working pressures and specific input powers W_d in discharges in all working gases. We thus conclude that the most important sterilizing factor of a discharge plasma is UV radiation. Experiments with a photoresist showed that UV radiation was emitted from plasmas at wavelengths no longer than ~220 nm. On the other hand, the fact that the experimental results obtained with the use of filters with limiting wavelengths of 160 and 120 nm are essentially the same leads to the conclusion that the lower limit on the radiation wavelength is 160 nm; in other words, sterilization by UV radiation with wavelengths in the range $160 \leq \lambda \leq 220$ nm is the most efficient.

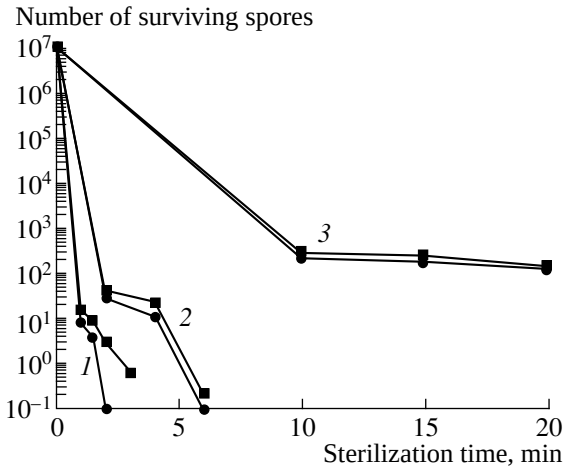

Fig. 5. Survivability profiles for the spores of Bacillus subtilis, which were obtained by counting the number of colonies during sterilization by the combined action of all of the sterilizing factors of the plasma (circles) and only by UV radiation from the plasma (squares) in discharges in (*1*) oxygen, (*2*) air, and (*3*) nitrogen at the pressure $P = 2 \times 10^{-1}$ torr and input power density $W_d = 3 \times 10^{-3}$ W/cm^3, the initial surface density of the spores being 10^7 spore/cm^2.

Note that the efficiency of sterilization by UV radiation from discharge plasmas is significantly higher than that by UV radiation from mercury lamps, which are routinely used in medical practice. For example, the duration of sterilization by UV radiation with the power $W_s \approx 100$ μW/cm^2 in a plasma sterilizer is five times shorter than that by UV radiation from a BUV-30 lamp with a much higher power of $W_s = 1500$ μW/cm^2. This mainly stems from the fact that the lamp emits UV radiation at significantly longer wavelengths (about 253 nm).

We point out here another important advantage of sterilization by UV radiation of plasma: since the sterilized products are immersed in the radiating plasma, the "shadowing" effect is essentially absent. Of course, this is primarily true of medical products free of holes narrower than the Debye radius of the plasma electrons (below, for brevity, the surfaces of such products will be referred to as free surfaces). The main sterilizing factor for products with complicated shapes (i.e., those with slits and holes narrower than the electron Debye radius) is chemically active neutral plasma particles rather than a more efficient UV radiation. Accordingly, it is very important to investigate the efficiency of sterilization by these particles. To do this, we developed a method aimed at studying sterilization by neutral plasma particles against the background of UV radiation, which is a more pronounced sterilizing factor. The essence of the method consists in protecting the sterilized objects by a fine metal grid, which reflected charged plasma particles because the grid cells were chosen to be narrower than their Debye radii, and by a screen, which was positioned behind the grid and was aimed at absorbing and reflecting UV radiation of the plasma. As a result, the test objects protected by both the grid and screen could be affected only by active neutral particles. We used grids with 0.01×0.01 mm cells and with a total area S_0 from 0.05 to 0.6 cm^2, the grid transmissivity being 80%. Geometrically, this system was arranged so that, over the entire range of the total grid area S_0, the particle density in the middle of a Petri dish was governed only by the balance between the particle influx through a hole of area S_0, the absorption of particles by the surface of the Petri dish, and by the particle outflux from the dish back to the discharge plasma. Consequently, as S_0 increases, the density of active neutral particles in the Petri dish should increase up to the plasma density in a certain critical area S_0. As a result, the sterilization time, which depends on the density of active particles, should decrease with increasing S_0 and should remain essentially unchanged above the critical value of S_0. Our experiments showed that the sterilization time actually decreased with increasing the hole area S_0 and became the shortest at $S_0 \geq 0.2$ cm^2. This shortest time is the time required to sterilize free surfaces by chemically active neutral plasma particles. In experiments with discharges in oxygen, nitrogen, and argon, the sterilization time was observed to depend on the hole area S_0 in an analogous manner. As in the case of discharges in air, the sterilization time was found to be the shortest at $S_0 \geq 0.2$ cm^2.

To compare the efficiency of sterilization by UV radiation from the plasma with that by chemically active neutral plasma particles, Fig. 6 shows the survivability profiles representative for discharges in oxygen

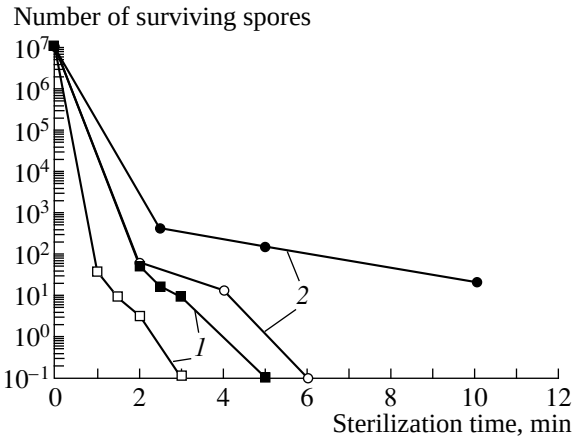

Fig. 6. Survivability profiles for the spores of Bacillus subtilis, which were obtained by counting the number of colonies during sterilization of free surfaces by active neutral plasma particles (closed symbols) and by UV radiation from the plasma (open symbols) in discharges in (*1*) oxygen and (*2*) air at the pressure $P = 10^{-1}$ torr and input power density $W_d = 3 \times 10^{-3}$ W/cm^3, the initial surface density of the spores being 10^7 spore/cm^2.

and air. We can see that, in the case of discharges in air, the duration of sterilization by UV radiation from the plasma is five to six times shorter than that by active neutral particles.

4. NUMERICAL MODELING

According to the experiments described above, the main role in sterilization of free surfaces is played by UV radiation, while charged plasma particles do not participate in the sterilization process (below, we will show that the plasma fluxes onto the sterilized surface are much less intense than the fluxes of UV photons and biologically active neutral particles).

The products with complicated shapes are sterilized mainly by the active neutral particles. In the case of discharges in oxygen, they are atoms, ozone molecules, and excited atoms and molecules. In the case of discharges in nitrogen, they are excited atoms and molecules.

In order to understand better what active particles are and to find the contents of the plasma, neutral plasma component, and radiation, we modeled glow discharges in nitrogen and oxygen under the operating conditions of a plasma sterilizer.

Our numerical model is based on the following kinetic equations for neutral and charged plasma components:

$$\frac{dN_i}{dt} = \sum_i k_i N_i + \sum_{i,\, j(i \le j)} k_{ij} N_i N_j + \ldots. \qquad (1)$$

where the first term on the right-hand side describes plasma processes in the approximation linear in the densities N_i of the plasma components, the second term accounts for binary collisions, and so on. The rate constants k_{ej} for binary collisions involving plasma electrons were determined from the expression

$$k_{ej} = \sqrt{\frac{2e}{m}} \int_0^\infty \varepsilon Q_{ej} f_0(\varepsilon) d\varepsilon, \qquad (2)$$

where ε is the electron energy (in units of eV), $e = 1.602 \times 10^{-12}$ erg/eV, m is the mass of an electron (in g), and $Q_{ej}(\varepsilon)$ is the cross section of the related collision process (in cm^2). The symmetric part of the EEDF, $f_0(\varepsilon)$, was found from the Boltzmann equation [10]

$$\frac{1}{n_e N}\sqrt{\frac{m}{2e}}\varepsilon^{1/2}\frac{\partial(n_e f_0(\varepsilon))}{\partial t} - \frac{1}{3}\left(\frac{E}{N}\right)^2 \frac{\partial}{\partial \varepsilon}\left(\frac{\varepsilon}{Q_T}\frac{\partial f_0(\varepsilon)}{\partial \varepsilon}\right)$$
$$-\frac{\partial}{\partial \varepsilon}\left[2\frac{m}{M}Q_T\varepsilon^2\left(f_0 + T\frac{\partial f_0(\varepsilon)}{\partial \varepsilon}\right)\right]$$
$$= S_{eN} + S_{ee} + A(\varepsilon) + L(\varepsilon). \qquad (3)$$

which was solved together with the kinetic equations (1). In (3), T is the gas temperature (in units of eV); n_e is the electron density; N_i is the density of gas molecules and Q_{iT} is the relevant transport cross section; S_{eN} and S_{ee} are the integral of electron–neutral inelastic collisions and electron–electron scattering, respectively; $A(\varepsilon)$ is the ionization term describing, in particular, the source of primary electrons; the term $L(\varepsilon)$ accounts for the electrons that escape to the anode; E is the electric field strength (in V/cm); and N is the net gas density.

The integral S_{eN} of electron–molecule inelastic collisions was chosen in the form

$$S_{eN} = \sum_j [(\varepsilon + \varepsilon_j) Q_{ej}(\varepsilon + \varepsilon_j) f_0(\varepsilon + \varepsilon_j) - \varepsilon Q_{ej}(\varepsilon) f_0(\varepsilon)] \qquad (4)$$

for discharges in nitrogen and in the form

$$S_{eN} = \sum_j [(\varepsilon + \varepsilon_j) Q_{ej}(\varepsilon + \varepsilon_j) f_0(\varepsilon + \varepsilon_j) - \varepsilon Q_{ej}(\varepsilon) f_0(\varepsilon)] - \varepsilon Q_d f_0(\varepsilon) \qquad (5)$$

for discharges in oxygen. In (4) and (5), Q_{ej} is the cross section for excitation and dissociation of molecules by UV photons with energies ε_j and Q_d is the cross section for dissociative attachment of electrons to O_2 molecules.

The expressions for the integral S_{ee} of electron–electron scattering and for the ionization term $A(\varepsilon)$ are presented in [11]. In our model, we adopted analogous expressions, but for the gases and energies of fast electron beams used in our experiments.

Since our measurements of the potential in glow discharges showed that the applied voltage of about 450 eV dropped preferentially across the cathode sheath with a thickness of about 1 cm, we assumed that the gas in a sterilizer was ionized by a beam of fast electrons with an energy of about 450 eV. In the main discharge plasma, the electric field was almost uniform and was approximately equal to 0.1 V/cm at a pressure of 0.1 torr. Consequently, the electrons escaping from the plasma to the anode can be described in the drift approximation. In the electron balance, we can neglect the electron losses due to electron recombination because the plasma density is low. These considerations allowed us to choose the following form of the term $L(\varepsilon)$, which describes the electrons escaping from the discharge chamber:

$$L(\varepsilon) = \frac{1}{3}\frac{E}{N^2}\frac{S_a}{V}\frac{\varepsilon}{N_i Q_{iT}(\varepsilon) + \sum_j N_j Q_{ej}(\varepsilon)}\frac{\partial f_0(\varepsilon)}{\partial \varepsilon}, \quad (6)$$

where S_a is the area of the anode surface and V is the volume of the discharge chamber.

The EEDF $f_0(\varepsilon)$ was normalized to satisfy the condition

$$\int_0^\infty f_0(\varepsilon)\sqrt{\varepsilon}\,d\varepsilon = 1. \quad (7)$$

We solved equations (1) and (2) numerically by the methods that were used and approved in [12, 13]. We assumed that the densities of all plasma components are uniform and applied the extended scheme of the kinetic processes listed in Tables 1 and 2 for nitrogen and oxygen, respectively. The UV radiation was assumed to be emitted only in transitions from the lowest resonant state to the vibrationally excited levels of the ground state. In the case of nitrogen, these transitions correspond to the Lyman–Berge–Golfield bands. The cross sections for elastic scattering of electrons by N_2 and O_2 molecules were taken from [14–16], and the cross sections for inelastic processes were taken from [16–22]. Some of the scattering cross sections and rate constants were taken from [22, 23].

Table 1

1	$N_2 + e \longrightarrow N_2^+ + e + e$
2	$N_2 + e \longrightarrow N_2(\alpha^1\Pi) + e$
3	$N_2 + e \longrightarrow N + N + e$
4	$N_2^+ + e \longrightarrow N + N$
5	$N_2(\alpha^1\Pi) + e \longrightarrow N_2^+ + e$
6	$N_2(\alpha^1\Pi) + e \longrightarrow N_2 + \hbar\omega_2$
7	$N + N + N \longrightarrow N_2 + N$
8	$N + N + N_2 \longrightarrow N_2 + N_2$
9	$N + \text{wall} \longrightarrow 1/2N_2$
10	$N + e \longrightarrow N^+ + e + e$
11	$N + e \longrightarrow N(3\sigma^4P) + e$
12	$N^+ + N + N \longrightarrow N_2^+ + N$
13	$N^+ + N + N_2 \longrightarrow N_2^+ + N_2$
14	$N(3\sigma^4P) + e \longrightarrow N^+ + e + e$
15	$N(3\sigma^4P) \longrightarrow N + \hbar\omega_1$
16	$N_2 + \hbar\omega_1 \longrightarrow N_2(\alpha^1\Pi)$
17	$N + \hbar\omega_1 \longrightarrow N(3\sigma^4P)$
18	$N_2^+ + e(\text{cathode}) \longrightarrow N_2$
19	$N^+ + e(\text{cathode}) \longrightarrow 1/2N_2$
20	$e \longrightarrow$ anode
21	e–e scattering
22	elastic scattering

5. NUMERICAL RESULTS AND COMPARISON WITH THE EXPERIMENT

Figure 2 shows representative profiles of the EEDF for discharges in nitrogen and oxygen (curves *1*, *2*). In the case of nitrogen, the EEDF is seen to be inverted ($df_0/d\varepsilon > 0$) in the energy range 2–4 eV because of the vibrational excitation of N_2 molecules; this result is confirmed by our experimental measurements (curve *3*). In the case of oxygen, the EEDF is monotonic because, first, the vibrational excitation cross section for O_2 molecules is much smaller than that for N_2 molecules and, second, in accordance with the experimental conditions, the EEDF was truncated at a low threshold energy corresponding to the electronic excitation of the molecular state $O_2(^1\Delta_g)$. Note that, to a considerable extent, the inversion of the EEDF in the case of nitrogen is also attributed to the weak electric field, which is characteristic of glow discharges at low pressures ($p \leq 0.1$ torr). In this situation, the EEDF is analogous to that observed at a certain time in a decaying plasma after switching off the electric field [8]. In the experiments with discharges in nitrogen [8], the EEDF was also observed to be inverted, which is explained by a sharp peak in the vibrational excitation cross section for N_2 molecules ($v = 1$–9) in the energy range 2–3.7 eV. At high pressures, the energy of fast electrons is too low for them to uniformly ionize the gas over the entire working volume; as a result, the electric field in the main discharge plasma increases. In this case, the EEDF becomes nearly Maxwellian and is similar in shape to that in [8, 23, 24] at the time $t = 0$ after switching-off of the electric field, because, according to (3), the electric field gives rise to diffusion in energy space.

Figures 7 and 8 depict the densities of the main plasma components versus pressure in the case of dis-

Table 2

1	$O_2 + e \longrightarrow O_2^+ + e + e$
2	$O_2(^1\Delta_g) + e \longrightarrow O_2^+ + e + e$
3	$O_2(b\,^1\Sigma_g^+) + e \longrightarrow O_2^+ + e + e$
4	$O_2(*) + e \longrightarrow O_2^+ + e + e$
5	$O_2(*) \longrightarrow O_2 + \hbar\omega_3$
6	$O_2 + \hbar\omega_3 \longrightarrow O_2(*)$
7	$O + e \longrightarrow O^+ + e + e$
8	$O_2 + e \longrightarrow O_2(^1\Delta_g) + e$
9	$O_2 + e \longrightarrow O_2(b\,^1\Sigma_g^+) + e$
10	$O_2 + e \longrightarrow O_2(*) + e$
11	$O_2 + e \longrightarrow O + O + e$
12	$O_2^+ + e \longrightarrow O + O$
13	$O_2 + e \longrightarrow O^- + O$
14	$O^- + O_2^+ \longrightarrow O + O_2 + e$
15	$O^- + O^+ \longrightarrow O + O + e$
16	$O^- + e \longrightarrow O + e + e$
17	$O^- + O_2 \longrightarrow O + O_2 + e$
18	$O^- + O \longrightarrow O + O + e$
19	$O + \text{wall} \longrightarrow 1/2O_2$
20	$O^+ + O + O \longrightarrow O_2^+ + O$
21	$O^+ + O + O_2 \longrightarrow O_2^+ + O_2$
22	$O^- + O_2(^1\Delta_g) \longrightarrow O_3 + e$
23	$O_3 + O_2(b\,^1\Sigma_g^+) \longrightarrow O_2 + O_2 + O$
24	$O_3 + e \longrightarrow O_2 + O + e$
25	$O_2(^1\Delta_g) + e \longrightarrow O + O + e$
26	$O_2(b\,^1\Sigma_g^+) + e \longrightarrow O + O + e$
27	$O_2^+ + e(\text{cathode}) \longrightarrow O_2$
28	$O^+ + e(\text{cathode}) \longrightarrow 1/2O_2$
29	$e \longrightarrow$ anode
30	*e–e* scattering
31	elastic scattering

charges in nitrogen and oxygen. It is seen from Fig. 7 that the densities of the primary products from electron–molecule reactions (i.e., plasma, atomic nitrogen and oxygen, and excited N_2 and O_2 molecules) are essentially pressure-independent. The reason for this is that, the higher the pressure of the discharge plasma, the higher the dissociation, excitation, and ionization energies at which the EEDF is truncated. Since the dissociation, excitation, and ionization rate constants k_{ej} defined in (2) are inversely proportional to the gas density, the total rate constants, which characterize the production of the corresponding components of the gas plasma and are defined as $k_{ej}N_{N_2, O_2}$, remain essentially unchanged.

Note that the densities of such biologically active components as atomic oxygen and excited oxygen molecules $O_2(^1\Delta_g)$ can be fairly high (about 10^{12} cm^{-3}). The density of the excited molecules $O_2(^1\Delta_g)$ is significantly higher than that of the excited N_2^* molecules (by three orders of magnitude) because of the low excitation energy ($\varepsilon = 0.95$ eV) of the $^1\Delta_g$ level of oxygen molecules. The densities of the secondary products from electron–molecule reactions, in particular, the number densities $N_{\hbar\omega_2}$ and $N_{\hbar\omega_3}$ of UV photons (about 10^3 cm^{-3}), are all low (Fig. 8). However, we must keep in mind that the densities do not affect the sterilization time, which is governed by the fluxes of the corresponding biologically active particles onto the substrate surface as well as by their penetrability and their sterilizing effect on the spores. The intensity $N_{\hbar\omega_2, \hbar\omega_3} \cdot c$ of the UV photon fluxes (3×10^{13} cm^{-2} s^{-1}) is more than one order of magnitude higher than the plasma flux intensity (about 10^{12} cm^{-2} s^{-1}), because the ambipolar diffusion rate in the plasma is low. The computed intensity of the UV photon flux and the computed plasma density both agree with those measured experimentally. Among the fluxes of active neutral particles, the most intense are those of oxygen atoms and excited molecules $O_2(^1\Delta_g)$ and $O_2(b\,^1\Sigma_g^+)$ (~10^{15}–10^{16} cm^{-2} s^{-1}), because the densities of these molecules are high. It is also seen from Fig. 8 that the densities of the excited nitrogen molecules increase with pressure (in contrast to the densities of the remaining neutral components). Since the sterilization efficiency is pressure-independent, we can conclude with a high degree of confidence that nitrogen plays an unimportant role in sterilization of the free surfaces of medical products. Presumably, this is attributed to the low nitrogen density (about 10^7 cm^{-3}) and low intensity (about 10^{11} cm^{-2} s^{-1}) of nitrogen fluxes.

The distributions of N_2 and O_2 molecules over vibrationally excited states are analogous to those in [23, 24]. Here, we do not focus on the vibrationally excited molecules $N_2(v)$ and $O_2(v)$, because they have the same valence as the N_2 and O_2 molecules in the ground state, which, however, do not affect the sterilization process, no matter how high their densities.

The densities of the plasma components that affect sterilization (UV photons, O atoms, and the excited molecules $O_2(^1\Delta_g)$ and $O_2(b\,^1\Sigma_g^+)$) increase linearly as the discharge current increases. This result agrees with

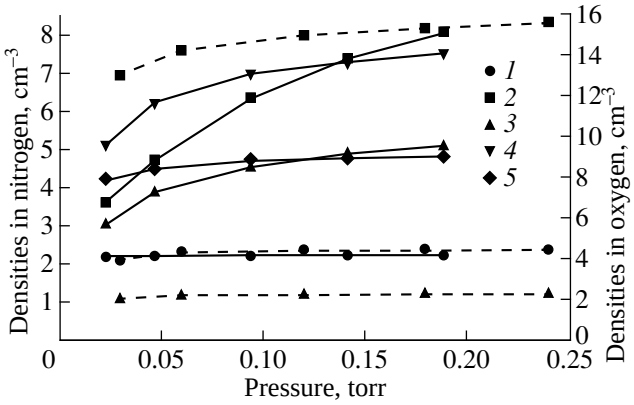

Fig. 7. Densities of the plasma components vs. pressure. The dashed curves correspond to nitrogen: (*1*) n_e, 10^8 cm^{-3}, (*2*) $N_{N_2^*}$, 2×10^9 cm^{-3}, and (*3*) N_N, 10^{12} cm^{-3}. The solid curves refer to oxygen: (*1*) n_e, 10^8 cm^{-3}, (*2*) N_O, 10^{12} cm^{-3}, (*3*) $N_{O_2(^1\Delta_g)}$, 10^{11} cm^{-3}, (*4*) $N_{O_2(b^1\Sigma_g^+)}$, 10^{10} cm^{-3}, and (*5*) $N_{O_2^*}$, 10^8 cm^{-3}.

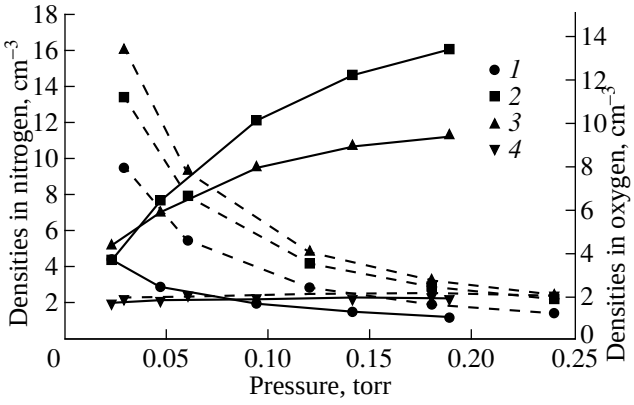

Fig. 8. Densities of the plasma components vs. pressure. The dashed curves correspond to nitrogen: (*1*) N_{N^+}, 10^4 cm^{-3}, (*2*) N_{N*}, 10^2 cm^{-3}, (*3*) $N_{\hbar\omega_1}$, cm^{-3}, and $N_{\hbar\omega_2}$, 10 cm^{-3}. The solid curves refer to oxygen: (*1*) N_{O_3}, 10^6 cm^{-3}, (*2*) N_{O^+}, 10^6 cm^{-3}, (*3*) N_{O^-}, 10^6 cm^{-3}, and (*4*) $N_{\hbar\omega_3}$, 10^3 cm^{-3}.

the measurements of the sterilization time, which was found to decrease in inverse proportion to the input power as the latter was increased. In other words, the sterilization efficiency increases linearly with increasing the discharge current. Note that the computed dependence of the plasma density on the discharge current agrees with that measured experimentally.

To conclude this section, note that, according to the results obtained, the main active particles that govern the efficiency of sterilization by discharge plasmas in oxygen and air are oxygen atoms and the excited molecules $O_2(^1\Delta_g)$ and $O_2(b^1\Sigma_g^+)$, although there are many other biologically active neutral particles in low-pressure glow discharges. This conclusion is supported primarily by a comparison between such parameters as the densities of different plasma components and the intensities of their fluxes, as well as between the dependences of these parameters on the pressure and discharge current. Since the density of biologically active particles in discharges in N_2 is much lower than that in discharges in O_2, sterilization in nitrogen requires longer time intervals in comparison with sterilization in oxygen.

6. CONCLUSIONS

The data obtained in our experiments allow us to draw the following conclusions:

(i) In the sterilization of free surfaces by discharge plasmas, the main role is played by UV radiation emitted from the plasma in the wavelength range from about 160 to about 220 nm.

(ii) The efficiency of sterilization by UV radiation from the plasma is significantly higher than that by UV radiation from sources that are routinely used in medical practice.

(iii) Medical products with complicated shapes are primarily sterilized by chemically active neutral plasma particles.

(iv) The duration of sterilization of free surfaces by active neutral particles in discharge plasmas in oxygen and air is two to six times longer than that of sterilization by UV radiation.

Our numerical modeling showed that, among the active neutral components in a discharge plasma in oxygen, the densities of oxygen atoms and oxygen molecules excited to the 0.98- and 1.64-eV energy levels are the highest. These are the particles that govern the efficiency of sterilization of medical products with complicated shapes.

The computed plasma density, EEDF, and UV radiation flux density agree well with the experimental data. This is also true for the dependences of the sterilizing factors of a discharge plasma on the discharge parameters.

ACKNOWLEDGMENTS

This work was supported in part by the Center for Science and Technology of Ukraine, project no. 57.

REFERENCES

1. W. P. Menashi, US Patent No. 3.383.163.

2. R. Bersin, US Patent No. 3.410.776.
3. L. Szu-Min, Thesis D. Sc. (University of Texas at Arlington, 1986).
4. *Proceedings of the International Kilmer Memorial Conference on the Sterilization of Medical Products, Moscow, 1989*, p. 80.
5. G. G. Shishkin and A. G. Shishkin, in *Proceedings of the 12 International Conference on Gas Discharges and Their Applications, Greifswald, 1997*, Vol. 2, p. 783.
6. V. A. Khomich, I. A. Soloshenko, V. V. Tsiolko, *et al.*, in *Proceedings of the 12 International Conference on Gas Discharges and Their Applications, Greifswald, 1997*, p. 740.
7. V. A. Khimich, I. A. Soloshenko, V. V. Tsiolko, *et al.*, in *Proceedings of the Congress on Plasma Sciences, Prague, 1998*, p. 2745.
8. R. Hugon, G. Henrion, and M. Fabry, Meas. Sci. Technol. **7**, 553 (1996).
9. M. J. Druyvesteyn, Z. Phys. **64**, 790 (1930).
10. J. P. Shkarofsky, T. W. Johnston, and M. P. Bachynski, *The Particle Kinetics of Plasmas* (Addison-Wesley, Reading, 1966; Atomizdat, Moscow, 1969).
11. P. M. Golovinskiĭ and A. I. Shchedrin, Zh. Tekh. Fiz. **59** (2), 51 (1989) [Sov. Phys. Tech. Phys. **34**, 159 (1989)].
12. A. I. Shchedrin, A. V. Ryabtsev, and D. Lo, J. Phys. B **29**, 915 (1996).
13. V. P. Goretskiĭ, A. V. Ryabtsev, I. A. Soloshenko, *et al.*, Zh. Tekh. Fiz. **63** (9), 46 (1993) [Tech. Phys. **38**, 762 (1993)].
14. R. Higgins, C. J. Noble, and P. G. Burke, J. Phys. B: At. Mol. Opt. Phys. **27**, 3203 (1994).
15. R. D. Hake and A. V. Phelps, Phys. Rev. **152** (1), 70 (1967).
16. A. V. Elitskiĭ, L. A. Palkina, and B. M. Smirnov, in *Transport Phenomena in Weakly Ionized Gases* (Atomizdat, Moscow, 1975), Chap. 5.
17. J. M. Ajello, J. Chem. Phys. **53**, 1156 (1970).
18. C. J. Gillant, J. Tennyson, B. M. McLaughlin, and P. G. Burke, J. Phys. B: At. Mol. Opt. Phys. **29**, 1531 (1996).
19. J. T. Fons, R. S. Schappe, and C. C. Lin, Phys. Rev. A **53**, 2239 (1996).
20. H. C. Straub, P. Renault, B. G. Lindsay, *et al.*, Phys. Rev. A **54**, 2146 (1996).
21. E. J. Stone and E. C. Zipf, J. Chem. Phys. **58**, 4278 (1973).
22. W. Hwang, Y.-K. Kim, and M. E. Rudd, J. Chem. Phys. **104**, 2956 (1996).
23. G. Gousset, C. M. Ferreira, M. Pinheiro, *et al.*, J. Phys. D: Appl. Phys. **24**, 290 (1991).
24. V. Guerra and J. Loureiro, J. Phys. D: Appl. Phys. **28**, 1903 (1995).

Translated by G. V. Shepekina